

AUTOMATIC BRAIN TUMOUR SEGMENTATION OF MAGNETIC RESONANCE IMAGES (MRI) BASED ON REGION OF INTEREST (ROI)

ANGULAKSHMI M. *, LAKSHMI PRIYA G. G.

School of Information Technology and Engineering, VIT University,
Vellore campus, Vellore - 632 014, Tamilnadu, India

*Corresponding Author: angulakshmi.m@vit.ac.in

Abstract

Segmentation is one of techniques used for classifying brain tissues in Magnetic Resonance Image (MRI) for identifying anatomical structures in the brain. The automated brain tumour segmentation remains challenging and computationally intensive because tumour appears in different size and intensity. In this paper, we have proposed a method for fast and automatic segmentation of tumour from Region of Interest (ROI) identified in MRI. ROI is a smaller portion of the image containing tumour. In the first step, tumour slices are identified using bilateral asymmetry property of the brain. In the second step, the ROI is identified using quadtree decomposition and similarity detection based on coefficient computed with gray level intensity histograms. In the third step, only the ROI is segmented using spectral clustering method rather than considering the whole image. Experimental results on real-world datasets are carried and compared with the recent existing works which show better results in terms of accuracy and less processing time for segmentation

Keywords: Bilateral asymmetry, Brain tumour, Region of interest, Spectral clustering, Segmentation.

1. Introduction

The Brain tumour is a group of abnormal growth of the cells, in and around the brain. Tumours can be classified as benign and malignant. Brain tumours can have a variety of shapes and sizes as it can appear at any location and in different image intensities. The number of people who dies due to brain tumour increased over 300% for few decades. Early detection of the brain tumour is very important

Nomenclatures

$C^{(i)}$	Distance between centroid and the points in the image, pixels
$H_{L(I)}$	Normalised left hemisphere histogram of the image
$H_{R(I)}$	Normalised right hemisphere histogram of the image
MI	Mean Intensity of pixels
$W_{m,n}$	Sliding Window of size m, n

Abbreviations

BC	Bhattacharya Coefficient
CSF	Cerebrospinal Fluid
GM	Grey Matter
IC	Intersection Coefficient
MRI	Magnetic Resonance Image
ROI	Region Of Interest

for saving the life of the people and motivated us for further studies. Medical imaging [1] plays a significant role in diagnosis and treatment of the brain tumours, which helps to manage and diminish the effects of the disease. The main idea is to help radiologists in finding the tumour, to improve the accuracy of diagnostics, to reduce the workload of a doctor, to reduce the time of treatment, to reduce the opportunity of cancer missed due to unclear and overloaded data and improve inter- and intra-reader variability.

Magnetic Resonance Imaging [MRI] [2] is one of the most popular medical imaging techniques. This is because MRI is non-invasive (using no ionization radiation), and capable of showing various tissues at high resolution with good contrast. Another advantage of MRI is to produce multiple images of the same tissue region with different contrast visualization capabilities [3]. These multiple images provide useful additional anatomical information about the same tissue region. Complementary information from different contrast mechanisms helps researchers to study brain pathology more precisely. Moreover, MRI split the image into different tissues White Matter (WM), Grey Matter (GM) and Cerebrospinal Fluid (CSF) [4]. In dealing with MRI images, one of the most challenging problems is to segment tumour because tumour appears in different size and in different intensity. The tumour can be segmented manually and automatically. Manual segmentation is an expensive, time consuming and tedious task. Automatic detection of tumour helps the physicians to find lesions more accurately.

Many machine learning and mathematical method exist in detecting and segmenting the tumour automatically. One of the popular segmentation techniques is spectral clustering. Segmentation using spectral clustering [5, 6] is flexible to define the relationship between data point (i.e., similar or dissimilar). Spectral clustering can work well for any group of data points. Once the similarity matrix is defined, a Normalized or un-normalized Laplacian matrix is created and the eigenvectors and eigenvalues of the Laplacian are calculated. Finally, the k-means algorithm on the eigenvalues is used to cluster corresponding to the k-smallest eigenvectors resulting in k-clusters. The flexibility of spectral clustering can also be a burden in which there are infinite ways to group points. Similarity matrix needs to be defined to find the similarity between data points. For example, for 'n' data

points, it is needed to create similarity matrix of size $n \times n$ where i^{th} row and j^{th} column represent the similarity between i^{th} row and j^{th} column data points. The popular ways of defining similarity are Euclidean distance, a kernel function of the Euclidean distance, or a k nearest neighbours approach. The pairwise similarity matrix construction of spectral clustering is very expensive in terms of computation and matrix storage for large dataset. Generally, Eigenvector [7] computation for a matrix of size $n \times n$ requires $O(n^3)$ complexity. Therefore, it requires much time and memory storage for large dataset.

Detecting tumour at earliest is very important for treatment. For this, a method for automatic segmentation of tumour is proposed by detecting suspicious region (ROI) that contains the tumour. Rather than considering the whole image, ROI is processed by spectral clustering algorithm for segmenting tumour region from MRI image. ROI is usually much smaller than the original image. Hence, the size of similarity matrix is reduced.

2. Related Work

Based on graph theoretic perspective, the first image segmentation algorithm based on spectral clustering [5] was formulated and the normalised cut to segment the image was introduced. Malik et al., [6] segmented the gray scale images based on a combination of contour and texture cues by applying the normalized cut formulation. However, the scalability of spectral clustering to large datasets is restricted due to large size of affinity matrix. The fast approximate spectral clustering [8] method consider only the small set of representative points rather than the original image for spectral clustering. K-means algorithm is used to find the k- representative points in pre-processing stage. However, the representative point does not capture the cluster geometrical structures effectively. Low-rank approximation of large affinity matrices by Nystrom methods [9] is commonly used to reduce the time complexity with spectral clustering method. This method applies the Nystrom approximation to the graph Laplacian to perform clustering.

The performance is good compared with spectral clustering with original laplacian. However, Nystrom method suffers from scalability problems when the dataset is very large and when eigenvectors are not orthogonal. This affects the approximation result. Column sampling [10] by means of Nystrom method forms a low rank approximation method by using the correlations between the sampled columns and the remaining columns. The Nystrom method can reduce the time and space complexities significantly because only the portion of the full matrix is computed. However, constructing the similarity matrix between all data objects is not easy to accomplish. On other hand, Self-Tuning Spectral Clustering algorithm [11] uses the local scale to find distance between each point to find affinity matrix rather than single scale. However, distances to neighbours are calculated by Euclidian distance factor which does not provide high accuracy as the Gaussian kernel function.

Spectral clustering under a budget constraint [12] focus on the problem of performing clustering based on the query. Limited numbers of similarity matrix entries are queried using the above method. Hence, data is reduced for clustering. However, the computation of similarities is often expensive or noisy for many applications. Active Spectral Clustering via Iterative Uncertainty Reduction [13]

formulated an active learning algorithm for spectral clustering. The method measures similarities incrementally for those that remove the uncertainty in an intermediate clustering solution. However, the method described above does not address clustering accuracy and bottleneck memory use. Modified Simple Linear Iterative Clustering [14] which preserves the desirable discontinuity characteristics and Nystrom based spectral clustering method is used to reduce the memory requirement and the computational complexity. Local information based fast approximate spectral clustering [15] improves clustering result by considering local information among the data while maintaining the scalability with large dataset. Spectral clustering via sparse representation [16] exploits contextual information from sparse representation vectors to construct weight matrices for spectral clustering of high- dimensional data. Parallel spectral clustering on distributed system [17] parallelizes the memory and computation on distributed machines. However, the accuracy and speed of computation demand more machines and paralleling spectral clustering is more challenging.

Several methods have been used to detect tumour. One among them is based on asymmetry characteristic of brain MRI image. The pixel intensity symmetry exists for two cerebral hemisphere of the normal brain in MRI. Many Research studies show that the asymmetry of the two brain hemispheres clues for brain injury [18, 19]. To enhance the accuracy and diagnosis of brain tumour, many researchers have utilised the bilateral asymmetry of brain structure [20, 21]. In Pixel based Symmetry Analysis of an Axial T2 Weighted Brain MRI [22], Mean pixel value gradient is used to compare left and right half of the brain to detect the presence of tumour. In Brain tumour detection based on bilateral symmetry information method [23] checks to detect whether image is divided into symmetric axes or not. If divided into symmetric axes, tumour does not exist. In Hybrid algorithm using symmetry and active contour [24], the image is reflected, the difference is taken between original and reflected image. Finally, the active contour is applied to difference image to segment the tumour. Several type of research is done to detect tumour based on symmetric property of brain.

In this paper, aiming to reduce size of similarity matrix and to produce high segmentation accuracy, a method for automatic segmentation of tumour is proposed. The rest of this paper is organised as follows. The pre-processing of image is presented in Section 3. Tumour detection is presented in Section 4. Automatic identification of ROI is presented in Section 5. Tumour segmentation using spectral clustering is presented in Section 6. Algorithm is presented in Section 7 Experimental results in Section 8 and finally conclusion remarks are presented in Section 9.

3. Pre-processing of Image

Image pre-processing and enhancement stage is the first stage in the proposed method for analysis of medical images. This stage is used to reduce the noise and improve resolution contrast of the image. Several de-noising approaches can be used (Rafael C .Gonzalez & Richard Eugene Woods, 2008). The median filter [25] is one of the most popular de-noising methods which helps to reduce noise, improve the quality in an image and preserves the edges of the images. The median filter is sliding window filter which replaces the central value with the mean of all pixel values in the window. Filtered image $I(i, j)$ is defined by the following Eq. (1)

$$I(i, j) = \text{median}\{c, d\} \in W_{m,n}\{d(i+c, j+d)\} \quad (1)$$

where $W_{m,n}$ is a sliding window of size $m \times n$ with centre pixel at (i, j) . Original image is shown in Fig. 1 and filtered image is shown in Fig. 2.

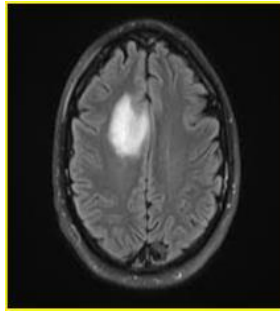


Fig. 1. Original image

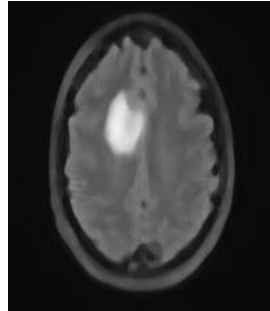


Fig. 2. Filtered image.

4. Tumour Detection

In the proposed method, the main idea in tumour detection is based on intensity asymmetry between the two brain hemispheres. First, the border of the brain is obtained by contour method. Dividing the brain into two hemispheres is achieved by finding the centre of mass of the brain. Line that passes through the centre of mass is taken as brain midline based on which the brain is divided into two hemispheres as shown in Fig. 3.

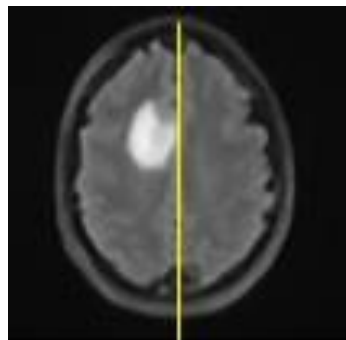


Fig. 3. Divide the MRI brain tumour image into two half.

In order to find symmetry of two hemispheres, various similarity measures based on gray level intensity histograms exists. In the proposed work to identify the better similarity measure that works well with MRI image, Bhattacharya coefficient similarity measures, Chi-square and Intersection based similarity measures are compared and the best of them are considered.

4.1. Bhattacharya similarity measure

The Bhattacharyya measure can be applied to any dataset without considering the distribution from which the data is sampled. Bhattacharyya Coefficient [BC][26] has already been used successfully in various computer vision applications, such

as object tracking, edge detection, and registration. Let $HL_{(t)}$ and $HR_{(t)}$ be the normalised histogram of left and right hemisphere of this image. The Bhattacharya Coefficient (BC) similarity measure can be defined in Eq. (2).

$$BC(HL_{(t)}, HR_{(t)}) = \sum HL_{(t)} * HR_{(t)} \quad (2)$$

The BC value is 1 for similar normalized histograms and the BC value is 0 for a dissimilar normalised histogram.

4.2. Chi-Square similarity measure

Chi Square Coefficient (CSC) [27, 28] similarity metric defined in the following Eq. (3).

$$CSC(HL_{(t)}, HR_{(t)}) = \sum (HL_{(t)} - HR_{(t)})^2 / HL_{(t)} + HR_{(t)} \quad (3)$$

When two normalised histogram are same, value of coefficient is large. When two normalised histograms are dissimilar, value of coefficient is small.

4.3. Intersection similarity measure

Intersection Coefficient (IC) [28] similarity metric defined in the Eq. (4).

$$IC(HL_{(t)}, HR_{(t)}) = \sum \min(HL_{(t)}, HR_{(t)}) \quad (4)$$

5. Region of Interest (ROI) Identification

Region of Interest identification is carried out by decomposing image into four equal quadrants, sub quadrants, and so on. In the proposed method, decomposition of the region into sub-quadrant occurs only for two levels to avoid over segmentation.

5.1. Procedure for Region of Interest(ROI) identification

ROI is identified by performing following procedure .For tumour slice, divide whole image into 4 quadrants as shown in Fig. 4. Compare top and bottom half's left quadrant with its corresponding right quadrant using the similarity measures. The dissimilar half (Top or Bottom) is further decomposed into 4 left sub quadrant and 4 right sub quadrant as shown in Fig. 5. Each (Top or Bottom) left sub-quadrant means intensity is compared with right sub-quadrant corresponding half. If sub-quadrant near midline of the brain has high mean, then (Top or Bottom) middle quadrant is labelled as ROI. If the sub-quadrant near the left border of the image has higher mean, (Top or Bottom) left-quadrant is labelled as ROI. If the sub-quadrant near the right border of the image has higher mean, (Top or Bottom) right quadrant is labelled as ROI.

ROI is one quadrant of an image, which passes through segmentation stage where tumour area is extracted. This gives us the opportunity to reduce the size of the image and increase the speed of processing in segmentation stage. The tumour detectable by this method depends on the threshold for the comparison of the

mean intensity of ROI. Higher values make it easier to detect small tumours, but only at the cost of a certain percentage of false positives (healthy quadrant are determined to contain tumour tissue). On another hand, a lower threshold prevents false positives. This is a trade-off problem as a degree of freedom for the designer depending on the application. On identifying ROI, the next phase is to segment the tumour portion from image.

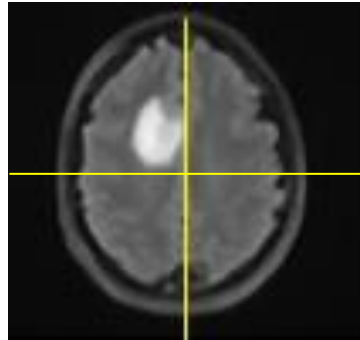


Fig. 4. Divide MRI brain tumour image into four quadrants.

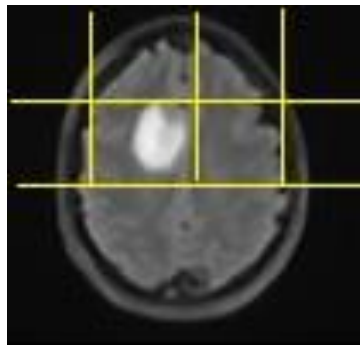


Fig. 5. Top left, top middle and top right quadrants of MRI brain tumour image.

6. Segmentation of Tumour

Segmentation of tumour can be done using Spectral clustering [5, 6]. The first step in spectral clustering is the construction of weighted graph where each node represents a pattern and each weighted edge specifies the similarity between two patterns. In the second step, the normalised Laplacian matrix of the weighted graph is obtained without loops and multiple edges. In the third step, the decomposition of Laplacian is done to find a low-dimensional representation of data. Then the first K Eigenvectors of Eigenvalues, form a matrix and K -means algorithm used to cluster them to obtain final clustering of data. The overall working of the proposed work is shown in a flowchart, Fig. A-1, in *Appendix A*.

7. Algorithm for Tumour Detection and Segmentation

The Algorithm for the proposed work is given in this section.

Input: Observed MRI brain image

Output: Segmentation of tumour area

Tumour slice identification

1. Pre-process the image using median filter
2. Divide the image into two hemispheres namely left hemisphere (L_H) and right half hemisphere (R_H) using centre of mass.
3. Using equation 2, compare the similarity measure S of L_H and R_H .
if $(S(L_H, R_H) == 1)$ label image as non-tumour slice.
Otherwise, label image as tumour slice

ROI identification and segmentation

4. Using quad tree decomposition, divide tumour slice into four quadrants T_L , T_R , B_L , and B_R namely top left quadrant, top right quadrant, bottom left quadrant and bottom right quadrant.
5. Compare the similarity measure S of T_L and T_R quadrant.
If $(S(T_L, T_R) == 1)$
 $D =$ Bottom half of the image
Otherwise $D =$ Top half of the image.
The D part of the image is further decomposed into 4 left sub quadrants L_{SQ} and 4 right sub-quadrants R_{SQ} using quadtree decomposition.
6. The pixel mean intensity(MI) for each sub-quadrant is calculated and compared with other half sub-quadrant
For all quadrant
If $MI(L_{SQ}(i)) > MI(R_{SQ}(i))$ then $R = L_{SQ}(i)$
Otherwise $R = R_{SQ}(i)$
7. If $R \in D$ lies near left boarder of image
Left quadrant of D is labelled as ROI.
Otherwise, R lies near right boarder of image
Right quadrant of D is labelled as ROI
Otherwise, middle quadrant of D is labelled as ROI
8. Segment ROI using spectral clustering.
9. End

8. Experimental Results

For our experiments, images are taken from National Biomedical Imaging Archives [NBIA] dataset [29]. The experiments involved axial brain MR image slices of 26 recent patient studies. Out of 26 images, 18 tumour slice and 8 non-tumour images are present. The dataset does not contain ground truth. The ground truths for the images are identified from expert manual segmentation. The proposed technique was developed in MATLAB15a version running under the windows-8 operating system with Intel R core(TM) i5-4500U CPU 2.30GHZ, and 8 GB of memory (RAM).

The metrics of sensitivity, specificity and accuracy are used to measure the performance of tumour detection. Sensitivity = $TP / (TP + FN)$, Specificity = $TN / (TN + FP)$, Accuracy = $(TN + TP) / (TN + TP + FN + FP)$, where TN is True Negative, TP is True Positive, FN is False Negative and FP is False Positive. The proposed method to detect tumour slice is done with three different histogram-based similarity measures namely Bhattacharya coefficient, chi square and Intersection similarity histogram measures. Out of which one similarity measure is selected their results are compared and shown in the Table 1. It can be observed that the proposed method produced a reasonable better result with Bhattacharya coefficient.

Table 1. Comparisons of different similarity measures.

	Bhattacharya	Chi-Square	Intersection
Sensitivity	94%	88%	83%
Specificity	88%	75%	87%
Accuracy	92%	84%	84%

The tumour detection accuracy of proposed method using Bhattacharya coefficient, as similarity measure is compared with Pixel based Symmetry Analysis of an Axial T2 Weighted Brain MRI [22] and Brain Tumour Detection Based on Bilateral Symmetry Information [23]. The comparison result is shown in the Table 2. Out of which the, proposed tumour detection method yields better result in terms of specificity, sensitivity and accuracy. All the methods are implemented using Matlab.

Table 2. Comparisons of segmentation process accuracy.

	Proposed Method	[22]	[23]
Sensitivity	94%	89%	91%
Specificity	88%	84%	85%
Accuracy	92%	88%	89%

In the proposed method, spectral clustering [6] is used to segment the tumour area from the ROI identified. In Fig. 6, Original image (a), Quadrant with high mean intensity (b), ROI(c) and segmented area (d) is shown. Spectral clustering is implemented using Matlab. For experiment purpose, the number of cluster k is taken as 2. The Nearest neighbour similarity function is used to construct similarity matrix. Then the normalised laplacian is constructed from the similarity graph. The computed vectors U_1, \dots, U_m from Laplacian are cluster into C_1, \dots, C_k cluster using K-means algorithm. The steps for K-means algorithm is as follows. The method first chooses K initial cluster centroids Q_1, Q_2, \dots, Q_k randomly. Repeat the following Eq. (5) and Eq. (6) until convergence. For every i , compute distance between centroid and the neighbour points using Eq. (5).

$$C^{(i)} = \min. \arg \left\| U^{(i)} - Q_{(j)} \right\|^2 \quad (5)$$

For each j , compute new centroid using Eq. (6)

$$Q_j = \sum_{i=1}^m \frac{(C_i = j)C^{(j)}}{(C_i = j)} \quad (6)$$

The performance of segmentation by spectral clustering is measured using clustering accuracy. This measure is defined in the Eq. (7)

$$Accuracy = \frac{\sum_{i=1}^n F(T_L, \text{map}(C_L))}{n} \quad (7)$$

where n is number of images, T_L is true labels and C_L is clustered labels. The map (\cdot) is a permutation function that is used map each obtained cluster label to a true label, and the optimal matching can be found by the Hungarian algorithm [30].

The 18 tumour MRI images are segmented from ROI using spectral clustering and their percentage of accuracy is compared with KASP [8] and Nystrom method [9]. For the above mention method namely KASP [8] and Nystrom [9], we have reused the code given in reference [31, 32] respectively for our dataset. The result of the comparison of accuracy is listed in the Table 3. Out of which the proposed method yield better accuracy.

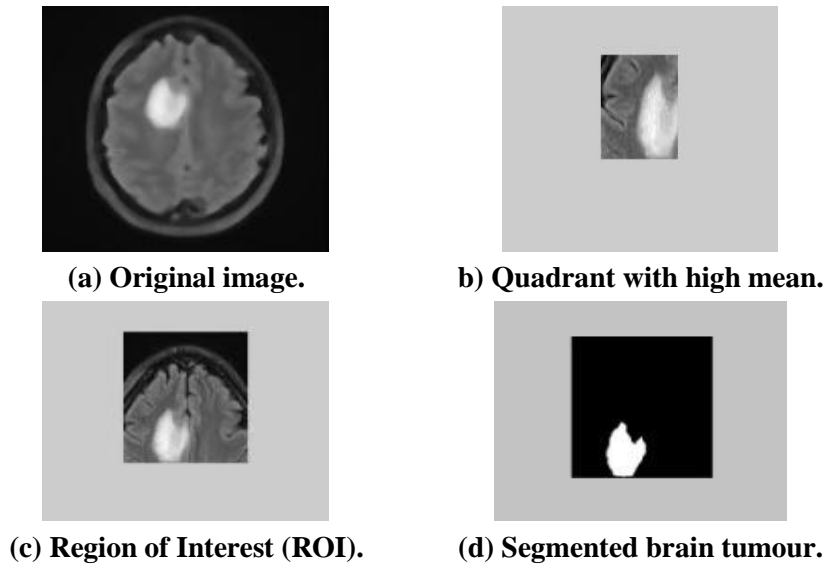


Fig. 6. The proposed method for brain tumour segmentation of MRI image based on ROI.

Table 3. Comparisons of segmentation process accuracy.

Methods	Accuracy
Nystrom method [9]	90.59
KASP [8]	94.31
The proposed method	95.15

The processing time of the proposed method is compared with KASP method [8] and Spectral clustering algorithms with Nystrom methods [9]. The measured results for processing time are listed in Table 4. From Table 4, it can be observed that the proposed method produced less processing time, compared to other recent existing method.

Table 4. Comparison of processing time.

Methods	Processing Time
KASP [8]	10.4 s
Nystrom [9]	12.6 s
Proposed method	10.2 s

9. Conclusion

The proposed method is a fast tumour detection technique that uses asymmetry property of the brain to enclose an anomaly from MRI image. The ROI is identified as tumour slice using quad tree based decomposition and asymmetry between those decomposed regions. The spectral clustering is then used to segment tumour from ROI. The proposed method is completely unsupervised, simple to implement and produced less processing time by obtaining tumour detection accuracy of about 92% and tumour segmentation accuracy of 95%. Further study would be done to detect tumours at the middle of the brain when both hemispheres are symmetry.

References

1. Tempany, C.M.; and McNeil, B.J. (2001). Advances in biomedical imaging. *Journal of American Medical Association*, 285(5), 562-567.
2. Selvanayagi, K.; and Karman, M. (2010). CAD system for automatic detection of brain tumour through magnetic resonance image-A review. *International Journal of Engineering Science and Technology*, 2(10), 5890-5901.
3. Kapur, T.; Eric, G.W.L.; William Wells, M.; and Kikinis, R. (1996). Segmentation of brain tissue from magnetic resonance images. *Medical Image Analysis*, 1(2), 109 -27.
4. Leemput, K.V.; Maes, F.; Vandermeulen, D.; and Seutens, P. (1999). Automated model-based tissue classification of MR images of the brain, *IEEE Transactions on Medical Imaging*, 18(10), 897-908.
5. Jianbo, S.; and Jitendra, M. (2000). Normalized cuts and image segmentation. *IEEE Transactions on Pattern Analysis and Machine Intelligence*, 22(8), 888-905.
6. Andrew, Y.N.; Jordan, M; and Yier, W. (2001). On spectral clustering: analysis and an algorithm. *Advances in Neural Information Processing Systems*. MIT press. Cambridge .USA. 849 - 856.
7. Harvey, R.E. (2002). *Linear Algebra. A Pure mathematical approach*. Springer.
8. Donghui, Y.; Ling, H.; and Michael, J.I. (2009). Fast approximate spectral clustering. *ACM Conference on Knowledge Discovery and Data Mining*, Paris. France.
9. Fowlkes, C.; Belongie, S.; Chung, F.; and Maik, J. (2004). Spectral clustering using the Nystrom method. *IEEE Transactions on Pattern Analysis and Machine Intelligence*, 26(2), 214-225.
10. Mu, L.; Xiao-Chen, L.; James, T.K.; and Bao-Liang, L. (2011). Time and space efficient spectral clustering via column sampling. *Proceedings of the IEEE Conference on Computer Vision and Pattern Recognition*, 2297–2304.
11. Zelnik-Manor, Z.; and Perona, P. (2004). Self-tuning spectral clustering, *proceeding of the 17th International Conference on Advances in Neural Information Processing System*, MIT Press and Cambridge, 1601-1608.
12. Ohad, S.; and Naftali, T. (2011). Spectral clustering on a Budget. *Proceedings of the 14th International Conference on Article Intelligence and Statistics*, Fort Lauderdale, FL, USA.

13. Fabian, L.; Wauthier, N.J.; and Michael, J.I. (2012). Active spectral clustering via iterative uncertainty reduction. *ACM International conference on Knowledge discovery and data mining, Beijing, China*. 1339-1347.
14. Baia, X.D.; Cao, Z.D.; Wanga, Y.B.; Yea, M.N.; and Zhua, L.B. (2014). Image segmentation using modified SLIC and Nystrom based spectral clustering. *Elsevier Journal of Optik*, 125(16), 4302-4307.
15. Jiang, Z.C.; Pei, C.; Qing, Y.D.; and Wing-Kuen, L. (2014). Local information-based fast approximate spectral clustering. *Elsevier journal of Pattern Recognition Letters*, 38(1), 63-69.
16. Sen, W.; Xiaodong, F.; and Wenjun, Z. (2014). Spectral clustering of high-dimensional data exploiting sparse representation vectors. *Elsevier Journal of Neurocomputing*, 35(5), 229-239.
17. Wen-Yen, C.; Yangqiu, S.; Hongjie, B.; Chih-Jen, L.; and Edward, C. Y. (2011). Parallel Spectral clustering in distributed system. *IEEE Transactions on Pattern Analysis and Machine Intelligence*, 33(3), 568-586.
18. Gilles, E.; Mc-Gregor, M.L.; and Levy-Clarke, G. (2003). Retinal haemorrhage asymmetry in inflicted head injury: a clue to pathogenesis. *Journal of paediatrics*, 143(4) .494-499.
19. Kumar, A.; Schmidt, E.A.; Hiler, M.; Smielewski, P.; Pickard, J.D.; and Czosnyka, M. (2005). Asymmetry of critical closing pressure following head injury. *Journal of Neurol. Neurosurgeon. Psychiatry*, 76(1), 570-573.
20. Lorenzen, P.; Joshi, S.; Gerig, G.; and Bullitt, E. (2001). Tumour-induced structural and radiometric asymmetry in brain images. *Proceedings in IEEE Workshop on Mathematical Methods in Biomedical Image Analysis*, 163-70.
21. Bergo, F.P.G.; Ruppert, G.C.S.; and Falcao, A. (2008). Fast and robust mid-sagittal plane location in 3D MR images of the brain. *Proceedings in International Conference on Bio inspired Systems and Signal Processing*, 92-99.
22. Kirti, R.B.; and Sarita, S.B. (2015). Pixel based Symmetry Analysis of an Axial T2 Weighted Brain MRI. *International Journal of Computer Applications*, 118(24), 9-14.
23. Narkhede, S.; Deven, S.; Vaishali, k.; and Sujata.K. (2014). Brain tumour detection based on bilateral symmetry information. *International journal of Engineering research and Applications*, 4(6), 98-103.
24. Mubbashar, S.; Jawad, H, K.; and Kalim, Q. (2014). A Hybrid Approach of Using Symmetry Technique for Brain Tumour Segmentation. *Computational and Mathematical Methods in Medicine*, Article ID 71278.
25. Prateek, K.G.; Pushpneel, V.; and Ankur, B. (2014). A Survey Paper on Various Median Filtering Techniques for Noise Removal from Digital Images. *American International Journal of Research in Formal Applied & Natural Sciences*, 7, 14-334.
26. Aherne, F.; Thacker, N.; and Rockett, P. (1997). The Bhattacharyya metric as an absolute similarity measure for frequency coded data. *Kybernetika*, 32(4), 1-7.
27. Priscilla, E.G.; and Michael, S.N. (1996). *A guide to chi-squared testing*. New York: John Wiley and Sons Inc.

28. Dietrich, V.W.; Mike, N.; and Etienne, E.K. (2002). An overview of similarity measures for images. *IEEE International Conference on Acoustics, Speech and Signal Processing*, 3317-3320.
29. National Cancer Institute. (2015). Retrieved September 2014, from <https://ncia.nci.nih.gov/ncia/>.
30. Papadimitriou, C.H.; and Stieglitz (1998). *Combinatorial optimization: algorithms and complexity*. New York. Dover and sons Inc.
31. Wen-Yen, C. (2011). Parallel Spectral Clustering in Distributed Systems. Retrieved September 2014, from <http://alumni.cs.ucsb.edu/~wychen/sc.html>.
32. Michael, I.J. (2004). Fast approximate spectral clustering. Retrieved August 2013, from <http://www.cs.berkeley.edu/~jordan/fasp.html>.

Appendix A

Flow chart of the proposed work

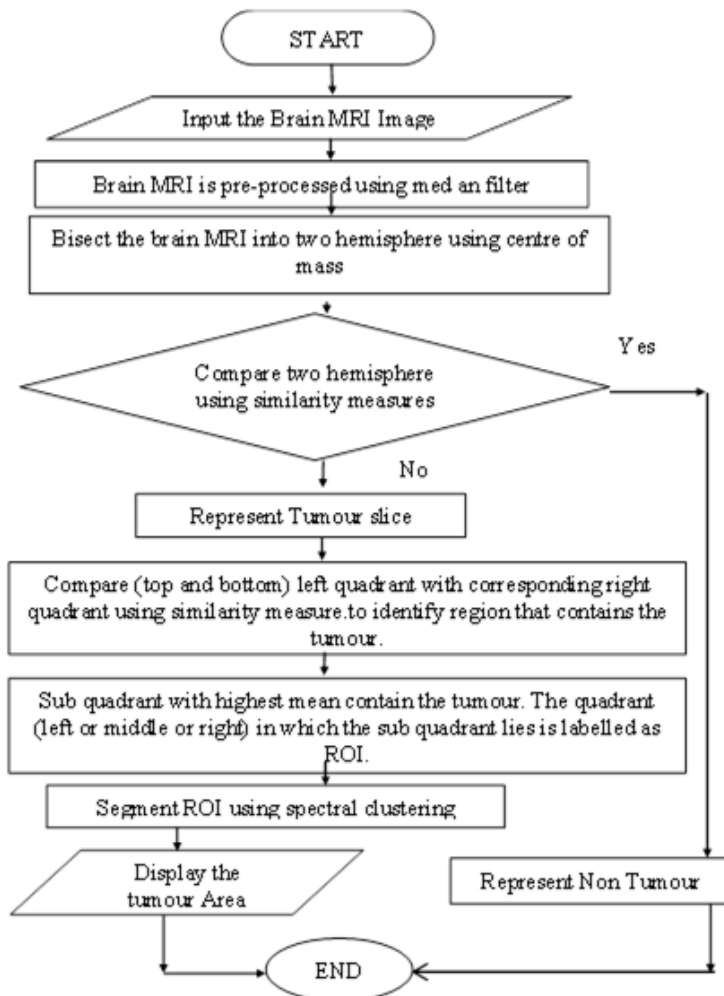


Fig. A-1. Flow chart of the proposed method.